ORIGINAL SCIENTIFIC PAPER

CROATICA CHEMICA ACTA

Croat. Chem. Acta **2015**, *88*(3), 297–306
Published online: December 30, 2015
DOI: 10.5562/cca2685

HKD 1926

Insight of the Iron Binding and Transport in Dke1 - A Molecular Dynamics Study

Hrvoje Brkić

Faculty of Medicine, J. Huttlera 4, HR-31000 Osijek, Croatia
Author's e-mail address: hbrkic@mefos.hr

RECEIVED: June 18, 2015 * REVISED: November 20, 2015 * ACCEPTED: November 25, 2015

Abstract: Acetylacetone dioxygenase from Acinetobacter johnsonii (Dke1) is a non-heme Fe^{2+} dependent enzyme which catalyzes the oxidative degradation of β-dicarbonyl compounds. It is a homotetramer with four active sites, each containing single metal ion. Since the active site is buried, knowledge on transport of the metal ion and reactants (products) is essential for understanding the enzyme mechanism. The goal of this study was to assess the influence of several point mutations on the enzyme activity. The point mutations of hydrophilic amino acid residues (Tyr70, Arg80 and Glu98) that were shown to be important for metal binding and reactants stabilization were of the particular interest. Computational study enabled us to determine the preferred metal ion binding sites as well, as the pathways it utilizes to enter the enzyme active site. Besides, influence of the point mutations on the hydrogen bond network within enzyme was determined.

Keywords: metaloenzyme, non-heme, iron, molecular dynamics.

INTRODUCTION

APPROXIMATELY one quarter to one third of all proteins require metals to carry out their functions.[1] One of such proteins is the Acetylacetone dioxygenase from *Acinetobacter johnsoii* (Dke1), which belongs to the family of Fe^{2+} dependent dioxygenases. It is a homotetramer[2] with each subunit organized in a single-domain β-barrel fold, characteristic for the cupin superfamily of proteins. Dke1 catalyzes the oxidative degradation of the β-dicarbonyl compounds[3,4] and for this purpose it needs Fe^{2+} ion. In the crystallographically determined structure the metal ion is coordinated with three histidines, while the molecular dynamics study showed that beside the histidines one glutamate could also take part in the metal ion coordination.[5] Although the Dke1 active site, besides the Fe^{2+} ion, can host several other metal ions, such as Co(II), Ni(II), Cu(II) and Zn(II), the enzyme is unable to catalyze the oxidative conversion of acetylacetone in their presence.[4] Until now only the effects of hydrophilic residues, placed in the second coordination sphere of the metal, have been investigated computationally, using the molecular dynamics (MD) simulations.[5] The main purpose of this study was to get insights into molecular mechanisms of Dke1, which haven't been demystified by now. Using computational methods the specific and non-specific metal ion binding sites are revealed and amino acid residues responsible for metal transport in and out of the Dke1 active site are identified. Additionally, the influence of hydrophilic residues mutations on the metal ion affinity and stabilization of ligand, i.e. 2,4-pentandione (PD), is investigated. Since the experimental data had suggested that hydrophilic residues in the active site pocket, Tyr70, Arg80 and Glu98, play a crucial role in the metal ion and substrate stabilization,[6] the point mutations of these amino acids were computationally prepared, and their influence to the protein structure and dynamics as well as on ligands binding and transport were investigated by computational methods. Previously published data reported that Dke1 has 2 metal binding sites,[7] but until now only one of them has been specified. In this study the alternative metal ion binding site(s) was determined and mechanism of the metal ion circulation within the protein was elucidated.

METHODS

System Preparation

The crystal structure of the substrate free Dke1 obtained from the PDB database[8] (pdb_id 3BAL) was used as the initial structure for the simulations. Several systems were prepared, as follows.

The point mutants Glu98Gln, Arg80Ala and Tyr70Ala, were prepared by editing the PDB file and using the module *tleap* (part of the AMBER12 package).[9] Water molecules determined in the crystal structure were removed, and zinc was replaced with the Fe^{2+} ion. Systems were parameterized using the AMBER[9] ff10[10] force field, GAFF[11] (General Amber force field), and the parameters for Fe^{2+} ion that were derived and tested earlier.[5,12] Parameters development was achieved with *ab initio* quantum mechanical calculations (using UHF method).[5] Equilibrium values for the bond distances, angles, and dihedrals, were determined, as well as their corresponding force constants. According to the experimental conditions,[2–5] the all simulations were performed at pH 7.5. Histidines were uncharged (singly protonated), aspartic and glutamic acids were negatively, and arginines and lysines positively charged. All other amino acid residues were neutral except the N and C terminal residues which were positively and negatively charged, respectively. Hydrogen atoms were also added by *tleap*, while protonation of the histidine imidazole ring (either Nδ1 or Nε2) was adjusted manually depending on the possibilities of hydrogen bond formation. The complexes with PD (2,4 pentandione) were constructed using the earlier determined Dke1-PD complex[5] as a template. For the complexes, besides the already mentioned force fields, the parameters derived earlier for the Fe^{2+} – substrate (PD) interactions were used.[5]

MD Simulations

Systems were placed in the truncated octahedron box filled with TIP3P[13] water molecules, with minimal distance of 9 Å between the solute atoms and the edge of the box. Neutralization was accomplished by adding Na^+ ions at the appropriate places on the protein surface.

Minimization of the systems was done in four, and equilibration in seven cycles, for details see previously conducted studies.[5,12] After minimization and equilibration each of the constructed mutants, (Arg80Ala, Glu98Gln and Tyr70Ala) as well as their complexes with PD, were submitted to 30 ns of unconstrained MD simulation. The time step during pre-equilibration, equilibration and the first 2 ns of the productive MD simulations was 1 fs, and remaining simulations were accomplished using the SHAKE algorithm[14] and 2 fs time step.

Besides the simulations where Fe^{2+} was described with both bonding and non-bonding parameters, several sets of MD simulations with the metal ion placed at different positions and described with non-bonding parameters solely were also performed. For the wild type and mutated proteins several sets of MD simulations were performed: a) with the Fe^{2+} ion initially placed into the active site (crystallographically determined pose), two sets of simulations, 16 ns and 30 ns each, b) with Fe^{2+} placed at the entrance of the water trafficking tunnels, 3 sets of simulations for the wild type enzyme (WT; 16, 6 and 3 ns long), 2 sets for the Tyr70Ala (16 and 5 ns) mutant and one for each the other two variants (16 ns)). Starting structures for these simulations were the final snapshots of the 5 ns long simulations with Fe^{2+} placed at (or close to) the entrance of the water trafficking tunnels, where one water molecule was replaced a with Fe^{2+}. Table ST1 (in Supplemental) contains list of all the preformed simulations with its respective duration.

The Binding Free Energy Calculations for Fe^{2+} Initially Placed in a Water Tunnel

The free energy for the hydrated Fe^{2+} binding to the enzyme was calculated using the MMPBSA[15] method as implemented in the AMBER package. Calculations were done on the 2-ns long final parts of the MD simulation trajectories. The concentration of the singly charged counterions was 0.1 M. Poisson–Boltzmann method was used to calculate the polar component of solvation, and non-polar component was determined using equation (1):

$$\Delta_{sol}H_{nonpolar} = \gamma \mathrm{SASA} \quad (1)$$

where γ is the surface tension with value of 0.0072 kcal mol^{-1} $Å^{-2}$. Solvent accessible surface area (SASA) was calculated using the MolSurf program.[16] The calculations were accomplished for the enzyme immersed into the solvent utilizing the solute dielectric constant of 4.0. As a ligand Fe^{2+} ion hydrated with two water molecules (the Fe^{2+} + two water molecules cluster) was considered, while the receptor was apo variant.

RAMD Simulations

Random acceleration molecular dynamics (RAMD)[17] simulations were used in order to determine the metal ion exiting paths and roughly estimate relative expulsion speed for the metal bound to different Dke1 variants. For each system (WT, Glu98Gln, Arg80Ala and Tyr70Ala) 4 runs were performed in each chain, altogether 54 runs. Simulations were done for 250 ps or until the distance between the protein and the Fe^{2+} centres of mass became greater than 30 Å. The time step was 1 fs, and the acceleration amplitude was 0.23 kcal/mol/Å/g. The direction of the force was kept for 40 time steps (40 fs). If a ligand did not move by more

Table 1. Percentage of the simulation time during which the hydrogen bonds between Glu98(OE1/2)-His104(NE2) and Glu11(OE1/2)-His104(NE2) exists, Simulations were performed on APO variants of Dke1

	WT	Tyr70Ala	Arg80Ala	Glu98Gln
Glu11(OE1/2)-His104(NE2)	0.07	0	7.6	0.2
Glu98(OE1/2)-His104(NE2)	56.3	73.8	19.1	5.4

than 0.01 Å during this period, a new direction was chosen randomly; otherwise the same force was applied for the next period of 40 time steps.

The structures were sampled every 1.0 ps and trajectories were analysed in details. Root mean square deviation, amino-acid fluctuations, water population of the enzyme active site, hydrogen bonds between amino acids of interest and other interesting features were monitored and analysed using the program *ptraj*[18] available within the Amber program suite.

Secondary Structure Analysis

The secondary structure of the simulated variants was determined by STRIDE WEB server.[19]

RESULTS AND DISCUSSION

In order to get insights into the molecular mechanisms of Fe^{2+} trafficking in and out of the enzyme active site, a set of MD simulations for the wild type protein and its single point mutants Tyr70Ala, Arg80Ala Glu98Gln and were performed: (i) of the Fe^{2+} free protein (apo enzyme), (ii) of the enzyme with Fe^{2+} bound in the active site, without and with applying random force, (iii) of the proteins with the metal ion located at the entrance of the water tunnel. The obtained trajectories were analysed and the Fe^{2+} migration paths, in and out of the protein, were determined.

(i) Simulations on APO Enzymes

A short, only 6 ns long, MD simulations of Dke1 wild type and its variants Tyr70Ala, Arg80Ala Glu98Gln and in their metal free form were performed in order to monitor influence of the point mutations on the overall protein structure and particularly on the active site structure. According to the calculated RMSD between the structure of the wild type enzyme and the mutants (1.7 Tyr70Ala, 2.4 Arg80Ala, 1.9 Glu98Gln) and the visual inspection it is clear that the mutations neither change the overall protein fold nor the secondary structure elements, ß sheets they are part of. However, due to differences in size, hydropobicity and other physico-chemical properties of the amino acid residues in the native enzyme and mutants their local environment, as well as protein flexibility, have changed. A comparison of the resulting trajectories revealed that Glu98 was more than 50 % of the simulation time H-bonded to His104 in the WT and Tyr70Ala mutant, while in the other two mutants this interaction is significantly weaker and it has disappeared during simulation, and both Glu98 and His104 were more flexible (see Table 1). Another carboxylate residue that was found rather close to the metal binding motif, Glu11 (from neighbour subunit), was generally not H-bonded to any of the metal binding histidines or hydrophilic triad residues (Tyr70Ala, Arg80Ala, Glu98Gln) and pointed away from the active site in all variants (see Table 1). A Figure 1 shows the optimized structure of the active site in different variants obtained after 6 ns of MD simulations.

(ii) MD Simulations with the Fe^{2+} Ion Bound into the Protein Active Site Defined by 3His

During MD simulations with the Fe^{2+} cofactor bound to the metal binding motif, which is according to the crystallographically determined Dke1 structure characterized with 3 histidines, Glu98 entered the metal ion coordination sphere

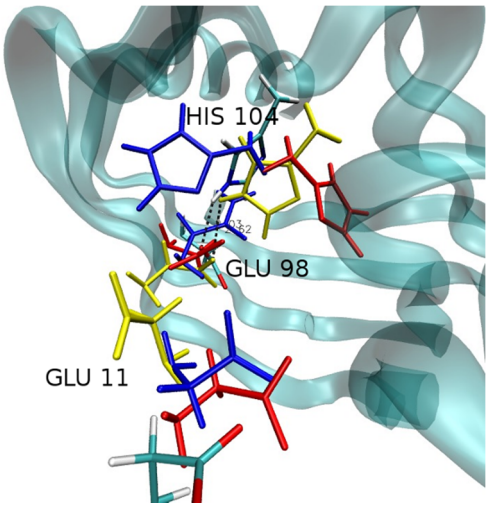

Figure 1. Glu11 (from neighbouur subunit) and Glu98 orientation; - in WT and in the Tyr70Ala mutant Glu98 is bound to the His104, while in other mutants it is free to move. His104, Glu98 and Glu11 are shown in stick representation with each variant coloured differently: WT by atom names, Tyr70Ala yellow, Arg80Ala red and Glu98Gln blue. Optimized structures obtained after 6 ns of MD simulations are shown. Figure is created using VMD.[20]

Table 2. Interactions between the metal ion and Glu/Gln98 during the simulations with the iron ion described with both bonding and non-bonding parameters. First two rows show the percentage of the time for Glu/Gln98-Fe^{2+} type of interaction. In last two rows distance (Å) between the iron and the carboxyl Glu/Gln side chain oxygens is given

	WT	Tyr70Ala	Arg80Ala	Glu98Gln
Monodentate coordination	73.5	65.2	32.6	45.4
Bidentate coordination	16.7	8.4	33.3	-
Average distance of closer oxygen	2.5	2.6	2.5	3.1
Average distance of farther oxygen	3.7	4.5	3.1	-

Table 3. Hydrogen bond analyses, percentage of the each bond persistent time is given. "Cplx" extension denotes complex with PD, „free" denotes ligand free protein with a metal ion in the active site and "T" denotes systems with Fe^{2+} initially placed into one of the water tunnels. X-not found; One letter notation for aminoacids is used to reduce space in table *data already published by *Brkić et al.*[5]

		E98Q cplx	E98Q free	E98QT	Y70A cplx	Y70A free	Y70AT	R80A cplx	R80A free	R80AT	WT* cplx	WT* free	WTT
GLY68 (O)	GLU98 (N)	99.9	99.5	9.9	74.6	75.0	X	99.5	99.9	99.9	74.0	100	X
GLY68 (O)	GLU98 (C)	63.5	X	13.9	2.9	13.0	X	X	X	X	X	5.0	X
GLU11 (OE12)	HIE104 (NE2)	43.5	X	4.9	24.4	X	X	X	100.0	23.5	3.0	84.0	11.1
ARG80 (NE)	GLU98 (OE1/2)	X	X	6.4	36.9	15.3	69.9	X	X	X	34.0	63.0	21.3
ARG80 (NH2)	GLU98 (OE1/2)	X	X	25.0	58.8	92.5	81.0	X	X	X	20.0	64.0	61.4
GLU98 HB(2,3)	GLU11 (OE1/2)	100.0	X	63.8	X	X	X	X	X	17.4	3.6	7.2	X
GLU98 (OE12)	HIE104 (NE2)	14.2	61.5	10.2	27.2	X	36.0	68.8	X	2.6	49.4	X	27.9

and most of the simulated time coordinated the metal ion either monodentately or bidentately in all variants (see Table 2). A typical orientation of Glu98 during the simulations is shown in Figure 2a. Most of the time during which Glu98 monodentately coordinated Fe^{2+} its other carboxyl oxygen was H-bonded to Arg80, in both the WT protein[5] and in the Tyr70Ala mutant (64 % and 92.5 % of the time, respectively).

Intriguingly, increased bidentate coordination of metal ion lead to reorientation of Glu11, and formation of the stable H-bond between Glu11 and His104 in the resting WT protein and the Arg80Ala mutant (during 84 % and 100 % of the simulation time, respectively, see Table 2 and Table 3). Glu11 changed its orientation and, showed a notable propensity of H-bonding to His104 in variants Glu98Gln and Tyr70Ala (Table 3). Differently, in the ligand

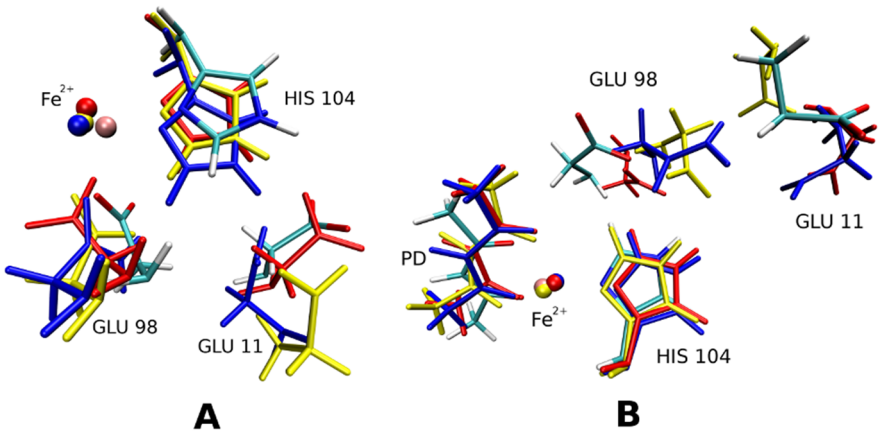

Figure 2. Orientation of residues Glu98, Glu11 (from neighbor subunit) and His104 in the different variants with the metal ion in the enzyme active site a) without substrate bound and b) with substrate bound. Stick representation colored by atoms represents WT system, red is Arg80Ala mutant, yellow is Tyr70Ala mutant and blue is Glu98Gln mutant.

Table 4. Persistence (% of the simulation time is given) of hydrogen bonds between residues Arg80 – His104, and Met117 – His 64 in simulations of Dke1-PD complexes. The iron ion was described with both bonding and nonbonding parameters

	WT	Tyr70Ala	Arg80Ala	Glu98Gln
Arg80(NH2) – His104(Ne2)	-	20	-	27
Met117(Ce) – His64(Nd1)	54	13	32	14

free protein this H-bond was mostly present in the WT protein and the Arg80Ala mutant. Further on it was noticed that in the complexes Tyr70Ala-PD and Glu98Gln-PD the residue Arg80 is H-bonded to His104 during about 20–30 % of the simulation time (see Table 4). Interactions between Glu11, His104 and Glu98 in the simulated complexes are shown in Figure 2b.

(iii) Simulations of the Systems with Substrate Bound to Dke1

The substrate, PD, binding to the active site induced expulsion of the Glu98 from the Fe^{2+} coordination sphere in all variants. During the simulations PD coordinated the metal ion bidentately, while Glu98 reoriented preserving its interactions with Arg80 in the WT protein (either with Ne, 34 %, or with NH2, 20 % of the simulation time) and in the Tyr70Ala mutant (with Ne, 37 %, and with NH2 59 % of the simulation time). In the variants Glu98Gln and Arg80Ala interactions between Arg80 and Glu98 were not established during the simulations. Arg80 NH2 interacted with Cδ of His104 during 28 % and 26 % of the simulation time in the Glu98Gln and Tyr70Ala mutants, respectively, while in other systems there was no such interaction. The interaction between Glu98 and His104 was the strongest in the Arg80Ala variant, follows WT, see Table 3.

To summarize, in the substrate bound complexes, the coordinate bond between Glu98/Gln98 and Fe^{2+} ion was lost in all variants, leading to a 3-His and diketonate ligated Fe(II) center. Instead, Glu98 interacted with His104 while intensity of this interaction varied among Dke1 variants (see text above and Table 3). Glu11 changed its orientation and, showed a notable propensity of H-bonding to His104 in variants Glu98Gln and Tyr70Ala (Table 3). Differently, in the ligand free protein this H-bond was mostly present in the WT protein and the Arg80Ala mutant. Further on it was noticed that in the complexes Tyr70Ala-PD and Glu98Gln-PD the residue Arg80 is H-bonded to His104 during about 20-30 % of the simulation time (see Table 4). Interactions between Glu11, His104 and Glu98 in the simulated complexes are shown in Figure 2b.

(iv) Fe^{2+} Detachment from the Active Site

In order to trace the putative trajectories of Fe^{2+} when migrating out of the active site set of MD simulations was performed in which the metal ion was described by nonbonding parameters only. The simulations were performed a) without and b) with an additional random force applied to the metal ion (details of the simulations are given in Materials and Methods).

(iv a) Fe^{2+} Migration out of the Metal Binding Site - no Additional Force

During MD simulations at room temperature with Fe^{2+} described only with its charge (1.5 e^+) and the van der Waals parameters migration of the metal ion out of the active site in all variants was noticed. At the end of the first 5 ns of MD simulations, about 2/3 of the metal binding sites were already empty in the Arg80Ala and the Glu98Gln variants, see Table 5.

The analysis of trajectories sampled for the WT protein and the Tyr70Ala mutant revealed that during 46 ns of MD simulations Fe^{2+} spent, on average, 30-35% of the simulation time in the active site (data averaged over all subunits). However, resistance of the metal ion to leave His62, His64 and His104 was significantly lower in the Arg80 and Glu98 variants (see Table 5). Such behaviour of metal ion is consistent with the binding free energies (precisely, the binding enthalpies) calculated using MM_PBSA method (see Table 6).

The metal ion migration can be traced in Figure 1S (see supplementary material) where its distance from the initial (3His, Glu) position is given. While in the Arg80Ala mutant Fe^{2+} ions left the metal binding site very fast, in the WT protein they migrated from and back to the active sites and rarely moved more than 3.5 Å away from their initial positions (Figure 1S, supplementary material).

In order to understand/rationalize mechanism of Fe^{2+} detachment from the active site metal coordination and the His104-Glu98-Arg80 interactions (see Figures 2S and 3S in supplementary material) were analysed. During the simulations Glu98 (in the case of the Glu98Gln variant,

Table 5. Percentage (%) of simulation time (averaged over all subunits) during which Fe^{2+} was present in the active site, *i.e.* coordinated with tree histidines and Glu98

Simulation time (ns)	Enzyme variant			
	WT	Arg80Ala	Glu98Gln	Tyr70Ala
first 5	69.1	36.9	32.0	55.1
46	34.8	9.1	16.9	28.3

Table 6. Relative energies (kcal/mol) for the binding of the hydrated Fe^{2+} (cluster of two water molecules and metal ion) to different Dke1 variants. Energy was calculated for each chain (A – D) using MM_PBSA approach. Energy for the metal binding to the C subunit of the WT enzyme was used as a referent

Variant	A	B	C	D	Average
WT	24.4	6.7	0.0	32.0	15.8
Tyr70Ala	19.4	46.9	42.4	35.4	36.0
Arg80Ala	44.5	21.0	27.4	37.2	32.5
Glu98Gln	60.2	43.6	45.3	31.0	45.0

Gln98) coordinates the metal ion either monodentately or bidentately. Ratio of bi/mono coordination is highest in the Arg80Ala mutant, follows the Tyr70Ala one (see Table 7). During simulations of the WT protein Glu98 was coordinating the metal ion in the active site (Fe^{2+} bound to three histidines) monodentately most of the time. At the same time the other carboxyl oxygen of the Glu98 was interacting via H-bond with Arg80. The metal migration out of the active site was accompanied with the Arg80-Glu98 separation. Due to reorientation of Arg80 (moving away from the metal centre), the H-bond between Arg80 and Glu98 broke resulting with increased mobility of Glu98. Subsequently Glu98 moved away from the metal binding site, and pulled the Fe^{2+} ion with itself (green and purple line in Figure 3S in supplementary material (WT) graphs). After that Glu11 reoriented, and took part in the metal ion coordination. The transient coordination of the metal ion by Glu11 and Glu98 was proposed to be important for Fe^{2+} transport in and out of the protein (see Figure 3). Since in the case of the Arg80Ala there is no Arg80 to constrain Glu98 motions it almost instantaneously (see Table 8), *i.e.* at the very beginning of MD simulation, pulled the metal ion out of the 3His binding site. Glu98 remained either bidentantely coordinated to the Fe^{2+} or it established hydrogen bond with His104 (see Figure 3S in supplementary material).

In the Glu98Gln variant no H-bond between Gln98 and either His104 or Arg80 was present during the simulation while the Fe^{2+} ion was in the active site. However, when the Fe^{2+} left the active site Gln98 hydrogen bonded to His104 (see Figures 1S and 2S i.e. subunit D in supplementary material).

Table 7. Percentage of simulation time during which Glu/Gln98 coordinatesFe^{2+}monodentately/bidentately. The iron ion was described by nonbonding parameters only

Coordination	WT	Tyr70Ala	Arg80Ala	Glu98Gln
Monodentate	97.5	87.5	77.3	70.8
Bidentate	2.5	4.8	22.7	0
ratio[bi/mono]	0.02	0.06	0.3	0

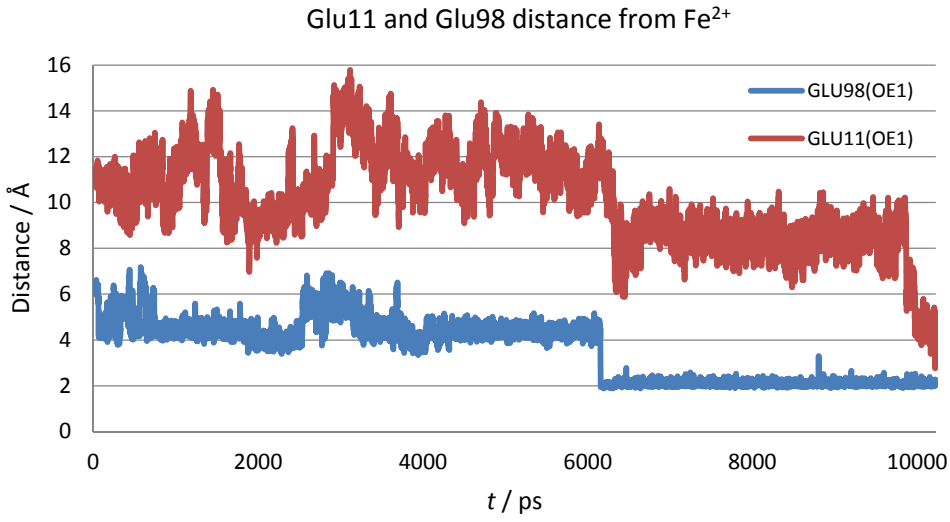

Figure 3. The Glu98(OE1) – Fe^{2+} and Glu11(OE1) – Fe^{2+} distances during 10 ns of MD simulations (the iron ion was described by nonbonding parameters only). The figure supports assumption that both Glu residues, Glu11 and Gu98, are important in the metal ion transportation, into and out of, the active site.

Table 8. Fe^{2+} positions (and their 'population') at the end of RAMD simulations. For each variant 16 RAMD simulations were performed. In the cases when the metal ion was expelled from the protein the number of expulsions through tunnel T2 (entrance defined by Glu11, see Figure 4) is given in square brackets

Fe^{2+} location	WT	Tyr70Ala	Arg80Ala	Glu98Gln
Out of protein [near Glu11]	2 [2]	4 [3]	5*	3 [2]
Glu11 neighbor sub.	3	8	4	6
Phe119 and Glu98	0	3	3	6
Thr107 and Glu78	7	0	0	0
Random	4	1	4	1

* in this mutants the water tunnels T1 and T2 cannot be distinguished (i.e. the Arg80 which is border between their entrances does not exist), however Glu11 still plays important role in of the metal ion expulsion

(iv b) The Detachment of Fe^{2+} from the Active Site by Applying Random Force

In another approach Fe^{2+} expulsion from the active site enhanced by the random force was simulated. In the presence of random force the metal ion detachment from the active site appeared in the much shorter time scale than noticed during 'regular MD' simulations (previous paragraph). Instead of one, a several simulations for the same 'computer cost' could be performed, result of which was the statistical distribution of the Fe^{2+} detachment pathways. The fate of the Fe^{2+} over a time range of 250 ps was monitored, and the end positions of the ions are summarized in Table 8.

In most cases the metal ion expelled from the 3His metal binding site ended close to Glu11 in all enzyme variants. In short, results showed that the mechanism of primary Fe^{2+} detachment out of the enzyme active site found by RAMD simulations is comparable to that described in the previous section. In the starting structure the Fe^{2+} was coordinated with 3 histidines and Glu98 (Figure 4S(A) in supplementary material), during the simulations the Fe^{2+} ion was pulled out of the active site by Glu98 but its coordination with His104 was still preserved (Figure 4S(B)). In the third step Glu98 moved Fe^{2+} away from His104 (Figure 4S(C)) in the direction of Glu11 from the neighbor subunit

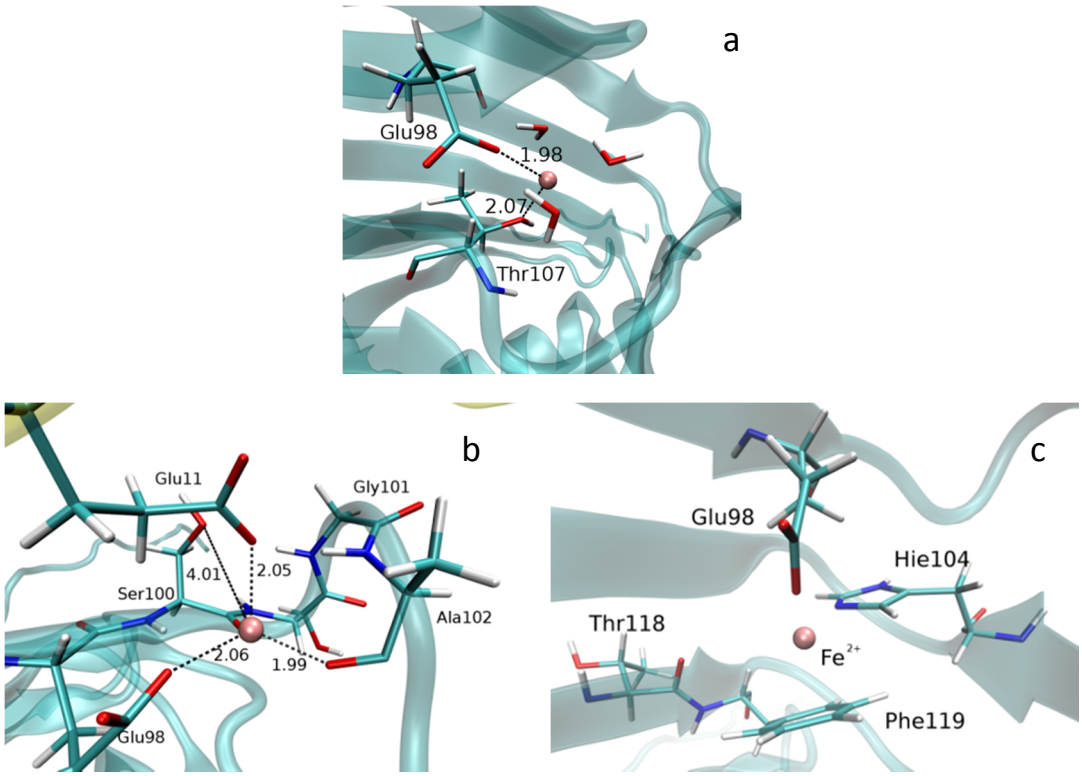

Figure 4. Positions of Fe^{2+} (pink ball) at the end of RAMD calculations: a) in the neighborhood of Thr107; b) close to Glu11 (from the neighbor subunit – the actually analyzed unit is given in transparent cyan, and neighbor subunit in yellow cartoon representation); c) next to Phe119.

Table 9. The position of the metal ion, initially placed in the water trafficking tunnels within 2.5 Å of the Tyr70 residue side chain oxygen, determined after 16 ns of MD simulations (this region is part of both water trafficking tunnels, T1 and T2).

System to which Fe was added	Unit A	Unit B	Unit C	Unit D
		Position of the Fe dikation at the end of MD simulations		
WT	CA	D	**A**	D2
WT**	**A1**	D	**A**	*S*
WT*	**A1**	D	**A1**	*S*
WT +Fe	D2	D2	D	D2
WT + ACAC + Fe	D	D	D	D
Tyr70Ala	D	CA	D	D2
Tyr70Ala *	D2	D	D	***E***
Arg80Ala	***E***	D	CA	D2
Glu98Gln	CA	D2	D2	D2

A = Fe^{2+} in the active site, coordinated with E98 and 3 His(s) ='ideal' position
A1 = Fe^{2+} in the active site, coordinated with E98 and 1 or 2 His
CA = with respect to its initial position Fe^{2+} moved in the direction of the active site, and ended close to the 'ideal position' (within ca 5 Å of it), but the coordination with E98 His(s) has not been established OR was established with only one of the 3His ligands
D = Fe^{2+} in the 'ALTERNATIVE' BINDING site, coordinated with E98 AND E11 from neighbour subunit
D1 = Fe^{2+} almost (close to) the 'ALTERNATIVE' BINDING site, coordinated with either E98 or E11 only
D2 = Fe^{2+} moved from the initial to the 'ALTERNATIVE' BINDING site direction, but still have not accomodated in it (cordination with neither E11 or E98 was established)
S = Fe^{2+} at the protein surface (solvated), close to/coordinated to Glu 85
E = Fe^{2+} escaped from the protein into the bulk water

(Figure 4S(D)) where it became accessible to the bulky solvent.

Alternatively, Fe^{2+} can be expelled into direction of Thr107 (the preferable path in the WT protein) as it is shown in Figure 4S(E) in supplementary material), where pink spheres represents motion of Fe^{2+} during RAMD. Remarkably, the preferred path for the Fe^{2+} ion in the WT enzyme was via a path that leads to Thr107 (Figure 4S(E)), where it rested, coordinated to the side chains of residues Glu78 and Thr107 while coordination to histidines was broken (see Figure 4). Notable, Thr107 has been reported to be crucial for Fe^{2+} binding.[6] Thr107 and Arg80/Glu78 belong to two adjacent beta strands. The Glu78 and Thr107 side chains interact electrostatically and so has a crucial role in stabilization of these beta strands (see Figure 5S in supplementary material).

In the Tyr70Ala and Arg80Ala variants the scenario depicted in Figure 4S was additionally facilitated by the increased Glu98 mobility. Upon Tyr70 and Arg80 mutation, respectively, Glu98 was less constrained and it reoriented more easily than in the WT protein leading the Fe^{2+} ion in a distinct directions. Since during the simulations of the Glu98Gln variant the hydrogen bond between Arg80 and Gln98 was not established (Table 3) Gln98 was more flexible than the Glu in the WT enzyme however, it was still able to guide Fe^{2+} out of the metal binding site, wherein in about 40 % of the cases metal ions were transferred to Glu11 of the neighbor subunit and in same amount of cases into direction of Phe119 (see Table 8 and Figure 4). Interestingly the Fe^{2+} coordination in the Glu98Gln mutant was not as tight as in the other variants.

In several cases the metal ion was expelled out of the protein. Expulsion of Fe^{2+} during simulations of the WT protein occurred through the water tunnel T2 (Table 8, see Figure S3 in previously published data[21] for definition of tunnels). As a consequence of lack of the Arg80 side chain a large exit tunnel, composed of exits of both water tunnels, was formed in the Arg80Ala mutant. As the result the Fe^{2+} ion ended in the bulk water, out of the protein more frequently than it was the case during simulations of the other Dke1 variants.

Data strongly suggest that the exit path for the metal ion is generally via tunnel T2, so passing beside Glu98 and Glu11. This tunnel was broadened during simulations of the all investigated variants. The alternative pathway, tunnel T1, comprising Thr107, was only occasionally used for the Fe^{2+} expulsion.

(v) Unrestricted Fe^{2+} Migration into the Protein

In a complementary approach Fe^{2+} was placed into the water tunnels in vicinity (up to 2.5 Å) of the Tyr70 side chain oxygen (which is part of both water trafficking tunnels)[5] and subjected to unrestricted MD simulations over 16 ns. In the wild type enzyme (apo form), Fe^{2+} was guided into/close to the 3-His 1-carboxylate metal binding site (defined as a <2.5 Å distance to all 3 histidine coordinated nitrogens) in 8 of 12 cases (see Table 9). In two cases Fe^{2+} got stuck on the protein surface, and in two cases it accommodated in the vicinity of Glu11. When either an Fe^{2+} ion or both, Fe^{2+} and substrate, were already bound in the binding site, the

Table 10. The mean secondary structures determined for the variants after MD simulations, averaged over all subunits. Content of helices and sheets deviates up to 4 % while content of turns within the proteins deviates up to 8 %

Variant	Helix (%)	Sheet (%)	Turn (%)
WT	7	48	21
Tyr70Ala	7	47	22
Glu98Gln	7	48	21
Arg80Ala	7	48	22

other Fe^{2+} ion predominantly ended at the nonspecific binding site, bound to Glu11/Glu98 (see Table 9).

Secondary Structure Analysis

In order to quantify effect of the point mutation on the overall protein structure we analyzed their secondary structure before and after each MD simulation using the web server STRIDE. According to the results it seems that the introduced point mutations do not have induced protein refolding, *i.e.* no significant changes of the protein secondary structure during simulations were noticed, see Table 10.

Discussion

The present study clearly speaks in evidence of biphasic binding of the metal ion to Dke1, which was predicted by Leitgeb *at al*.[7]

According to the results of RAMD simulations, the Fe^{2+} ion when expelled from the binding site could be trapped at different locations within the enzyme. However, the largest number the RAMD simulations ended close to Glu11 (3 times or (19 %) in WT; 4 in Arg80Ala (25 %); 6 in Glu98Gln (38 %); 8 in Tyr70Ala (50 %), Table 8 and Figure 4b), which can be considered as an alternative, low affinity binding site. The number of Fe^{2+} trajectories ending out of the protein was the smallest in the case of the Dke1-WT (only two of sixteen), indicating that the Dke1- Fe^{2+} complex is more stable than the mutated complexes.

In accord with the RAMD simulations the binding free energy calculations (see Table 6) revealed the neighborhood of Glu11 (form the neighbor subunit) as the second most favorable binding site for the Fe^{2+} ion (after the active site).

Detailed analysis of the metal ion coordination and His104-Glu98-Arg80 interactions during the simulations revealed importance of Glu98 in the ion transport. Further on, Arg80 and Tyr70, through their interactions with Glu98, also influenced the Fe^{2+} transport.

Results of the long unconstrained MD simulations for the enzyme variants (Table 5) indicated that presence of the metal ion in the active site is the shortest in Arg80 mutant.

Hydrogen bond analyses revealed relocation of the Gln98 side chain of the Glu98Gln variant in direction of the neighbor beta strand during the MD simulations. Such behavior of Gln98 is in favor of the metal ion translocation out of the active site in direction of Glu11 from the neighbor subunit. During the simulations of Tyr70Ala variant guanidine end of Arg80 established strong interaction with Glu98. As a result an ideal trap for the metal ion has been formed between the carboxyl groups of Glu98 and Glu11 from the neighbor unit. Arg80 to Ala mutation caused relocation of Glu11 from neighbor subunit closer to His104, enabling formation of the Glu11(OE1/2) – His104(NE2H/CD2H) H-bond (Table 1), while in the WT protein His104 was strongly interacting with Glu98, which was at the same time often interacting with Arg80, during the simulations. Figure 4S A-D indicate that Glu98, His104, Glu11 (from the neighbor subunit), and Arg80 interplay is crucial for the Fe^{2+} ion stabilization and transfer. Apparently Fe^{2+} affinity to bind to the glutamates carboxyl group is very high, since it spent the significant amount of simulations time coordinated either by Glu98 or Glu11, or both.

According to the computational results the metal ion could easier fluctuate between the active site and the alternative binding site next to Glu11 in the mutated (Tyr70Ala, Arg80Ala and Glu98Gln) enzymes than in the wild type. Yet, during the simulations of WT protein with Fe^{2+} initially placed in the water tunnel, the metal ion most often moved towards Glu11 (in 60 % simulations and in direction of the active site in 25 % simulations, see Table 9).

CONCLUSIONS

From the conducted computational analyses, mechanism of the Fe^{2+} trafficking in and out of the protein was elucidated. Interplay of Glu98, His104, Glu11 (from the neighbor subunit), and Arg80 residues is determined to be the most important for the Fe^{2+} transport. Also a place for the low affinity binding site is proposed, and it is in the vicinity of the Glu11 residue. Upon the point mutations of the hydrophilic residues Tyr70, Arg80 and Glu98 the metal ion is determined to be generally more flexible, so the role of the specified residues is shown to be important for metal stabilization in the active site.

Acknowledgment. The research was done in Physical Chemistry Department of Ruđer Bošković Institute in Zagreb, and Faculty of Medicine in Osijek. All MD simulations were done using Isabella computing cluster (http://www.srce.unizg.hr/isabella/) and Croatian National Grid Infrastructure (www.cro-ngi.hr).

REFERENCES

[1] K. J. Waldron, N. J. Robinson, *Nat. Rev. Microbiol.* **2009**, *7*, 25.

[2] G. Stranzl, Ph. D. Thesis, Institute of Chemistry, Karl Franzens University Graz, Graz, Austria, **2002**.

[3] G. Straganz, L. Brecker, H.-J. Weber, W. Steiner, D. W. Ribbons, *Biochem. Biophys. Res. Commun.* **2002**, *297*, 232.

[4] G. Straganz, A. Glieder, L. Brecker, D. Ribbons, W. Steiner, *Biochem. J.* **2003**, *369*, 573.

[5] H. Brkić, D. Buongiorno, M. Ramek, G. Straganz, S. Tomić, *J. Biol. Inorg. Chem.* **2012**, *17*, 801.

[6] G. D. Straganz, A. R. Diebold, S. Egger, B. Nidetzky, E. I. Solomon, *Biochemistry* **2010**, *49*, 996.

[7] S. Leitgeb, G. Straganz, B. Nidetzky, *Biochem. J.* **2009**, *418*, 403.

[8] S. Velankar, C. Best, B. Beuth, C. H. Boutselakis, N. Cobley, A. W. Sousa Da Silva*, et al.*, *Nucleic Acids Res.* **2010**, *38*, D308.

[9] D. Case, T. Darden, T. Cheatham III, C. Simmerling, J. Wang, R. Duke*, et al.*, *AMBER 12*, **2012**, San Francisco.

[10] Y. Duan, C. Wu, S. Chowdhury, M. C. Lee, G. Xiong, W. Zhang*, et al.*, *J. Comput. Chem.* **2003**, *24*, 1999.

[11] J. Wang, R. M. Wolf, J. W. Caldwell, P. A. Kollman, D. A. Case, *J. Comput. Chem.* **2004**, *25*, 1157.

[12] H. Brkic, B. Kovacevic, S. Tomic, *Mol. Biosyst.* **2015**, *11*, 898.

[13] M. W. Mahoney, W. L. Jorgensen, *J. Chem. Phys*. **2000**, *112*, 8910.

[14] J.-P. Ryckaert, G. Ciccotti and H. J. Berendsen, *J. Comput. Phys*. **1977**, *23*, 327.

[15] B. R. Miller III, T. D. McGee Jr, J. M. Swails, N. Homeyer, H. Gohlke, A. E. Roitberg, *J. Chem. Theory Comput*. **2012**, *8*, 3314.

[16] M. L. Connolly, *J. Appl. Crystallogr*. **1983**, *16*, 548.

[17] S. Lüdemann, C. Lounnas, R. Wade, *J. Mol. Biol.* **2000**, *303*, 797.

[18] D. R. Roe, T. E. Cheatham III, *J. Chem. Theory Comput*. **2013**, *9*, 3084.

[19] M. Heinig and D. Frishman, *Nucleic Acids Res*. **2004**, *32*, W500.

[20] W. Humphrey, A. Dalke and K. Schulten, *J. Mol. Graphics* **1996**, *14*, 33.

[21] http://static-content.springer.com/esm/art:10.1007/s00775-012-0898-8/MediaObjects/775_2012_898_MOESM1_ESM.docx

Supplementary material:

	Duration [ns]	Variant	Description
1	16	WT	Fe^{2+} ion initially placed into the active site
2	30		
3	16		Fe^{2+} placed at the entrance of the water trafficking tunnels
4	6		
5	3		
6	5		
7	16x0.25		RAMD
8	6		APO-enzyme
9	6		Second Fe^{2+} placed at the water trafficking
10	8		Second Fe^{2+} placed at the water trafficking and ligand bound
11	30		With bonding parameters
12	16	Tyr70Ala	Fe^{2+} ion initially placed into the active site
13	30		
14	16		Fe^{2+} placed at the entrance of the water trafficking tunnels
15	5		
16	5		
17	16x0.25		RAMD
18	6		APO-enzyme
19	30		With bonding parameters
20	16	Arg80Ala	Fe^{2+} ion initially placed into the active site
21	30		
22	16		Fe^{2+} placed at the entrance of the water trafficking tunnels
23	5		
24	16x0.25		RAMD
25	6		APO-enzyme
26	30		With bonding parameters
27	16	Glu98Gln	Fe^{2+} ion initially placed into the active site
28	30		
29	16		Fe^{2+} placed at the entrance of the water trafficking tunnels
30	5		
31	16x0.25		RAMD
32	6		APO-enzyme
33	30		With bonding parameters

Table ST1. List of all simulations for each Dke1 variant, with respective duration of simulation

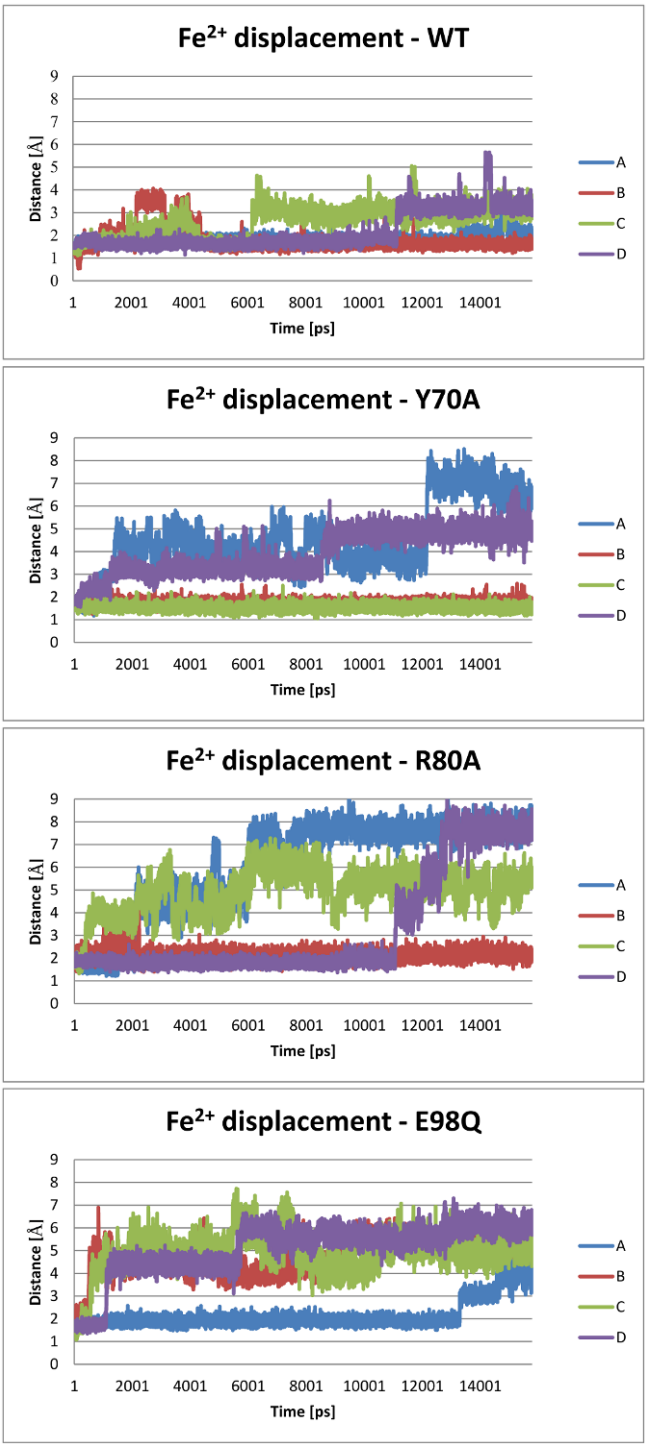

Fig. 1S Distances of metal ion from its initial position in four subunits during the first 16 ns of MD simulations at room temperature

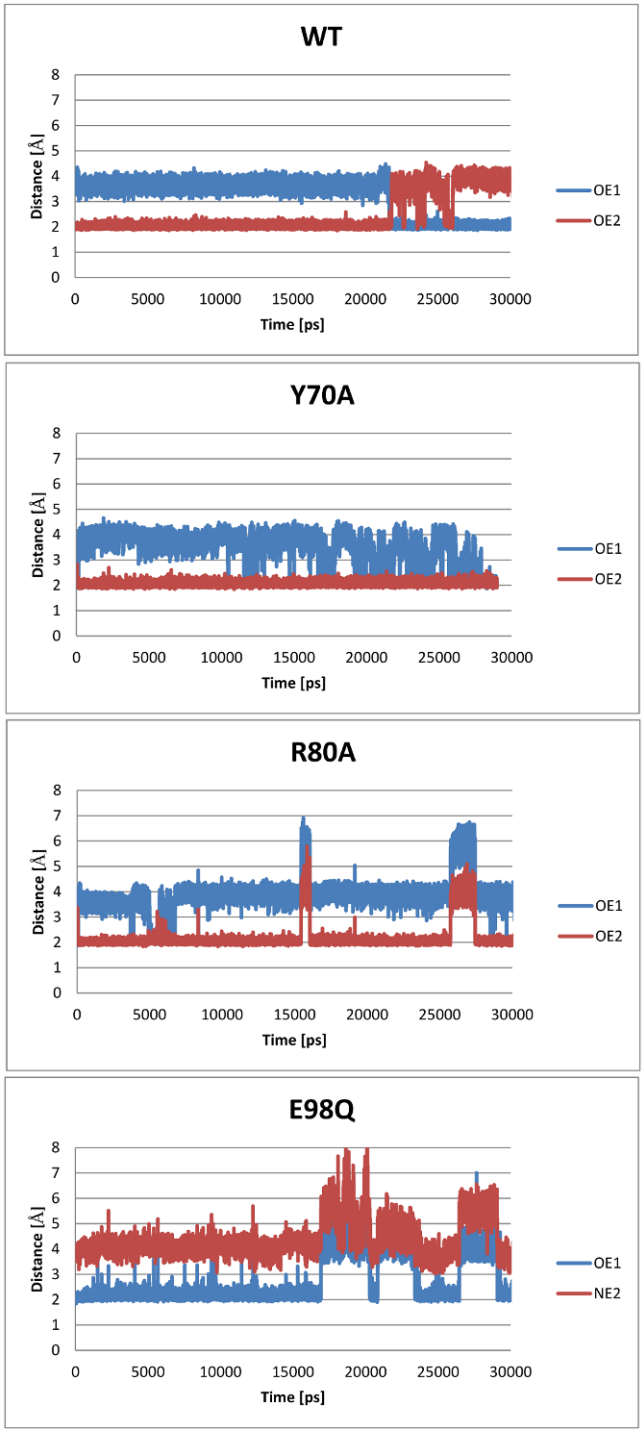

Fig. 2S The Glu/Gln98 – Fe^{2+} distances in one representative subunit (D) during first 30 ns of MD simulations at room temperature

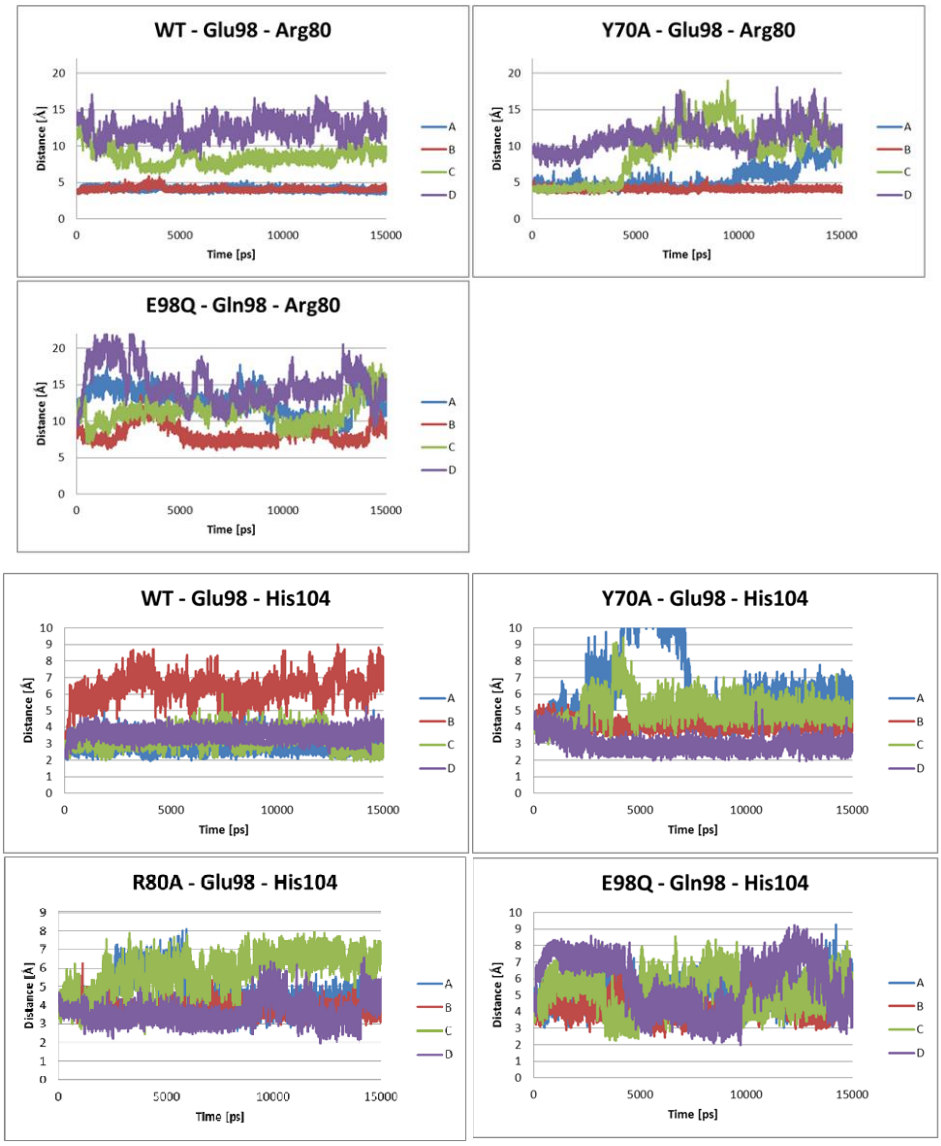

Fig. 3S Distances between Glu98 and Arg80 (and between His104 and Glu98) in four subunits during the first 15 ns of MD

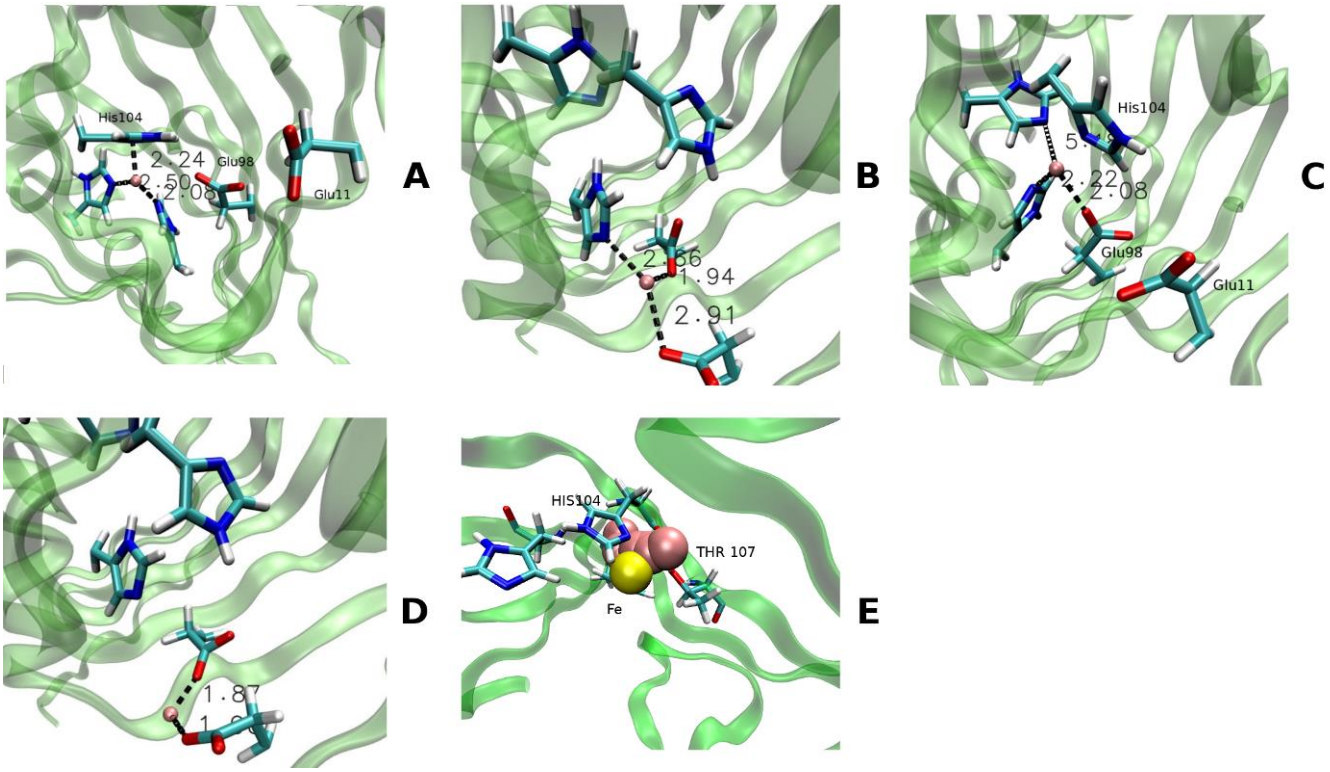

Fig. 4S Representation of a Fe^{2+} detachment trajectory. The β strands shown in green transparent representations, the amino acid side chains in colored sticks, and Fe^{2+} as a pink ball (except in E, where it is represented by yellow sphere). Black dashed lines represent bonds shorter 2.5 Å.

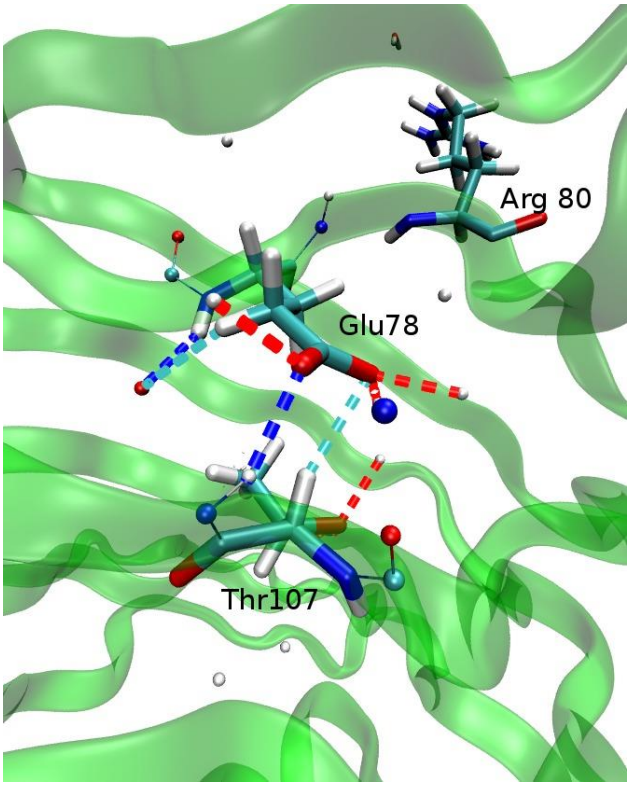

Fig. 5S Connections between Thr107 and Glu78 belonging to two adjacent beta strands.

Figure legends

Fig. 1S Distances of metal ion from its initial position in four subunits during the first 16 ns of MD simulations at room temperature

Fig. 2S The Glu/Gln98 – Fe^{2+} distances in one representative subunit (D) during first 30 ns of MD simulations at room temperature

Fig. 3S Distances between Glu98 and Arg80 (and between His104 and Glu98) in four subunits during the first 15 ns of MD

Fig. 4S Representation of a Fe^{2+} detachment trajectory. The β strands shown in green transparent representations, the amino acid side chains in colored sticks, and Fe^{2+} as a pink ball (except in E, where it is represented by yellow sphere). Black dashed lines represent bonds shorter 2.5 Å.

Fig. 5S Connections between Thr107 and Glu78 belonging to two adjacent beta strands.